Combustion and Flame 160 (2013) 473–485

Contents lists available at SciVerse ScienceDirect

Combustion and Flame

journal homepage: www.elsevier.com/locate/combustflame

An experimental and numerical study of surface chemical interactions in the combustion of propylene over platinum

Jihad Badra [a,*], Assaad R. Masri [a], Chenlai Zhou [b], Brian S. Haynes [b]

[a] School of Aerospace, Mechanical and Mechatronic Engineering, The University of Sydney, NSW 2006, Australia
[b] School of Chemical and Biomolecular Engineering, The University of Sydney, NSW 2006, Australia

ARTICLE INFO

Article history:
Received 12 June 2012
Received in revised form 17 October 2012
Accepted 24 October 2012
Available online 17 November 2012

Keywords:
Catalytic combustion
Reactivity limits
Homogeneous and heterogeneous reactions
Propylene on platinum
Micro-combustion

ABSTRACT

This paper describes the reactivity of premixed propylene/air mixtures co-flowing around a flat, vertical, unconfined, rectangular, platinum plate. Measurements and detailed computational fluid dynamics (CFD) calculations are performed to study the effects of varying the temperature of the incoming mixture (T_{jet}), its equivalence ratio (Φ) and the Reynolds number (Re), on the reactivity limits, platinum surface temperature and species distributions adjacent to the plate. A detailed surface chemical mechanism is implemented in the CFD calculations while pyrometry and gas chromatography are used, respectively, for surface temperature measurements and gas analysis.

It is found that the platinum plate temperature peaks at slightly rich propylene/air mixtures ($\Phi = 1.3$) when flameless combustion (defined by the presence of reactions on the plate without a gaseous flame) is observed. While the lean reactivity limits over platinum are lower than those for gaseous propylene/air mixtures, the rich limits are also lower than those of the gas phase alone and a sharp drop in the surface temperature is observed at $\Phi = 1.4$. This sharp transition to extinction may be due to surface contamination by soot precursors. Carbon monoxide (CO), and hydrogen (H_2) appear in low quantities at certain flow conditions. Consistent with other fuels, the streamwise profiles of species confirm the presence of two reacting zones along the plate, namely: (i) the leading edge zone where high gradients of species mole fractions are observed and (ii) the trailing zone where the profiles are more flat and stable. Numerical simulations show broad agreement with measurements up to $\Phi = 1.4$ but fail to reproduce the sharp transition to extinction hence overpredicting the rich reactive limits. Major species such as O_2, C_3H_6, and CO_2 are in good agreement with the measured mole fractions while some discrepancies are noted for CO and H_2. Differential molecular as well as thermal diffusions are found to be significant hence disrupting the atomic balance and leading to leaner mixtures in the vicinity of the plate.

1. Introduction

In earlier publications [1,2], the interactions between platinum and a series of alkanes were studied experimentally using the simple configuration of a vertical, rectangular, unconfined platinum plate surrounded by a co-flowing stream of premixed reactants. Compressed natural gas (CNG), ethane, dimethyl ether (DME), liquefied petroleum gas (LPG), and butane were examined over a range of equivalence ratios, jet temperatures, and Reynolds number; and measurements of surface temperatures as well as species composition obtained from probe sampling and gas chromatography analysis were reported. The following key conclusions were drawn: (i) the reactive limits of the fuels over platinum are broader than those corresponding to the gas phase alone with the rich limits being broadest for CNG followed by DME, ethane, propane, and butane [1,2]; (ii) peak surface temperatures obtained in flameless mode (surface reaction without a visible flame) are similar for all fuels, and (iii) amongst the five fuels studied, CNG showed the poorest fuel conversion resulting in high concentrations of fuel residue as well as CO close to the platinum surface [1].

This paper extends the knowledge base to propylene using the same experimental configuration, measurement techniques and range of studied parameters. Additionally, the measurements are compared to calculations that use a detailed surface mechanism for propylene over platinum [3]. A key impediment to enhancing current understanding of the interactions between hydrocarbon fuels and surface catalysts lies in the shortage or reliable surface chemistries for catalysts interacting with various fuels. Surface chemistries on platinum have become available for hydrogen [4], CO [5], methane [5], ethane [6] and more recently propylene [3]. Such mechanisms, however, may not be optimized for a wide

* Corresponding author. Address: CCRC, Al-Kindi Building, Mechanical Engineering, King Abdullah University of Science and Technology, Jeddah 23955-6900, Saudi Arabia.
E-mail address: jihad.badra@kaust.edu.sa (J. Badra).

0010-2180/$ - see front matter © 2012 The Combustion Institute. Published by Elsevier Inc. All rights reserved.
http://dx.doi.org/10.1016/j.combustflame.2012.10.021

range of conditions as was evident from earlier calculations reported for methane on platinum [2]. The current work highlights similar issues for propylene and calls for additional research in this field.

Combustion over platinum has been investigated by others using various micro-reactor configurations and with fuels such as H_2 [7–11], CO [12], CH_4 [13–17], and C_3H_8 [13,18,19]. The group of Mantzaras employed a range of diagnostic methods including Raman scattering [18] and concluded [18] that: (i) the Lewis number (Le) effects are significant such that methane with a Le number close to unity shows "higher transverse transport towards the catalytic surface" [18] and hence wider stability limits than propane, and (ii) the surface chemistries of CO and H_2 tend to decouple at high temperatures while for a lower temperature range around 710–720 K, CO(s) coverage of the surface tends to inhibit reaction [12]. Smyth et al. [20,21] have studied the interactions of methane and propane with platinum on a simple configuration of a flat plate positioned in a co-flowing fuel/air mixture. They reported measurements of temperature as well as selected species sampled from close to the plate and analyzed using gas chromatography and mass spectroscopy (GC–MS). They conclude that the reactive layer along the plate can be nominally split into three zones [20,21]: zone I very close to the leading edge characterized by sharp temperature increase accompanied with fast depletion of gaseous reactants, zone II where the surface temperature plateaus at a high value and reactants concentrations remain, and zone III further downstream where extinction of the non-adiabatic reaction occurs and a replenishment of reactants from the free stream was observed.

The development of rigorous surface chemistry remains very limited to a selected range of fuels and surfaces with methane/air combustion over platinum having received serious attention [5,22–25]. The mechanisms for hydrogen and carbon monoxide combustion on platinum are considered to be subsets of methane chemistry but both fuels have also been investigated separately [26]. The chemistry of higher hydrocarbons as well as oxygenated fuels on platinum is either non-existent or not as well developed. The chemistry of propane/air combustion over platinum is generally modeled as a one-step reaction with Langmuir–Hinshelwood kinetics [25,27,28] and the individual steps are not discussed. This approach has recently been used by Stefanidis and Vlachos [19] and Karagiannidis et al. [13]. It should be noted that the development of reliable thermodynamic data bases for surface species would aid significantly in the generation of micro-kinetic mechanisms for surface reactions.

This paper presents a numerical and experimental investigation of the interactions of propylene–air mixtures with a platinum surface. Parameters such as the equivalence ratio, mixture temperature, and Reynolds number are varied. The surface chemistry developed by Chatterjee et al. [3] is employed. Surface temperature measurements are performed using two-color infrared pyrometer and the species analysis is completed using the gas chromatography (GC).

2. Experimental set up

The configuration used earlier [2] for fuel/air mixtures co-flowing around a flat vertical unconfined platinum plate is adopted here for propylene. Hence, only a brief description of the experimental set up, shown in Fig. 1 is provided here and more details can be found in [2]. The 30 cm long heater (TEMPCO) can achieve exit temperatures up to 600 °C for Reynolds numbers ranging from 250 to 1500 and with equivalence ratios that range from $\Phi = 0$ to $\Phi = \infty$. The Reynolds number reported here are arbitrarily based on the burner's exit diameter ($D = 23$ mm) and the corresponding approach velocities are also provided for convenience. An arrangement of meshes is used within the tube and a sintered bronze plate is placed at the exit plane to keep the flow exiting the tube laminar ($Re < 2000$) and uniform in both temperature and velocity. Gas issuing from the 23 mm-ID stainless steel tube flows over both sides of the platinum plate, which has a width of 6 mm, length of 20 mm and a thickness of 0.25 mm. The platinum plate is held by two pointy ceramic pins as shown in Inset A of Fig. 1. It should be noted that the ceramic was machined to minimize the area of contact with the platinum plate so that the heat losses are negligible.

All measurements reported here ensure that the platinum plate is fully engulfed by the mixture issuing from the jet so that the results are neither dependent on the separation from the leading edge of the nozzle nor on the nozzle diameter. A PID controller (Novus N1200) is used to regulate the temperature of the mixture at the exit plane of the burner. The parameters varied during the experiments are (i) the equivalence ratio, Φ, of the fuel mixture co-flowing over the platinum, (ii) its temperature at the jet exit plane, T_{jet}, and, (iii) its Reynolds number, Re_d, which is based on the 23 mm-ID of the fuel tube. High purity (99%) propylene is used to perform this experiment. The qualitative burning characteristics observed here for propylene are similar to those described earlier for other hydrocarbons [2]. A blow torch is used for ignition and any established flame is subsequently blown off. One of the following scenarios may then prevail:

- *Extinction*: The platinum plate cannot sustain reaction and its temperature stabilizes at that of the unreacted co-flowing mixture.
- *Flaming combustion:* Subsequent to the initial ignition and blow-off, a flame re-ignites, propagate back and stabilize on the exit plane of the fuel tube. No measurements are made with this mode of combustion since the plate is shrouded with hot combustion products.
- *Flameless combustion:* No flame is re-ignited subsequent to the initial blow-off but the platinum plate remains reactive. While in some cases the plate may be clearly red-hot, this does not have to be the case since surface reactions may be maintained at much lower temperatures as will be evident from the results presented here.

The surface temperature of the platinum was measured using a two-color infrared pyrometer (Mikron M90R) that covers a range between 700 °C and 2000 °C. The infrared pyrometer was calibrated prior to performing the experiments and an accuracy of about 99% in measuring the temperatures of an object with known temperatures was reported. For surface temperatures below 700 °C, an estimate is obtained by using a type-K thermocouple to measure the gas temperature just downstream the platinum plate.

2.1. Gas sampling and analysis methodologies

Gas samples are extracted from 16 different locations along the streamwise and transverse directions of the platinum plate as shown in Inset B of Fig. 1 and detailed in Table 1. The coordinates (axial, radial) of few sampling locations are also shown in Inset B of Fig. 1. All of the measurements are taken along the middle of the platinum plate. For each case, a sample of unreacted mixture is taken from the jet exit plane and analyzed. A NewEra single syringe pump NE-1010 is used to control the flow rates in and out of the syringe which is equipped with an SGE valve and a Hamilton stainless steel needle (5 cm long, 0.31 mm-ID, and 0.57 mm-OD) connected to the valve. The needle is positioned near the platinum plate with the aid of a magnifying lens. Using a controlled suction

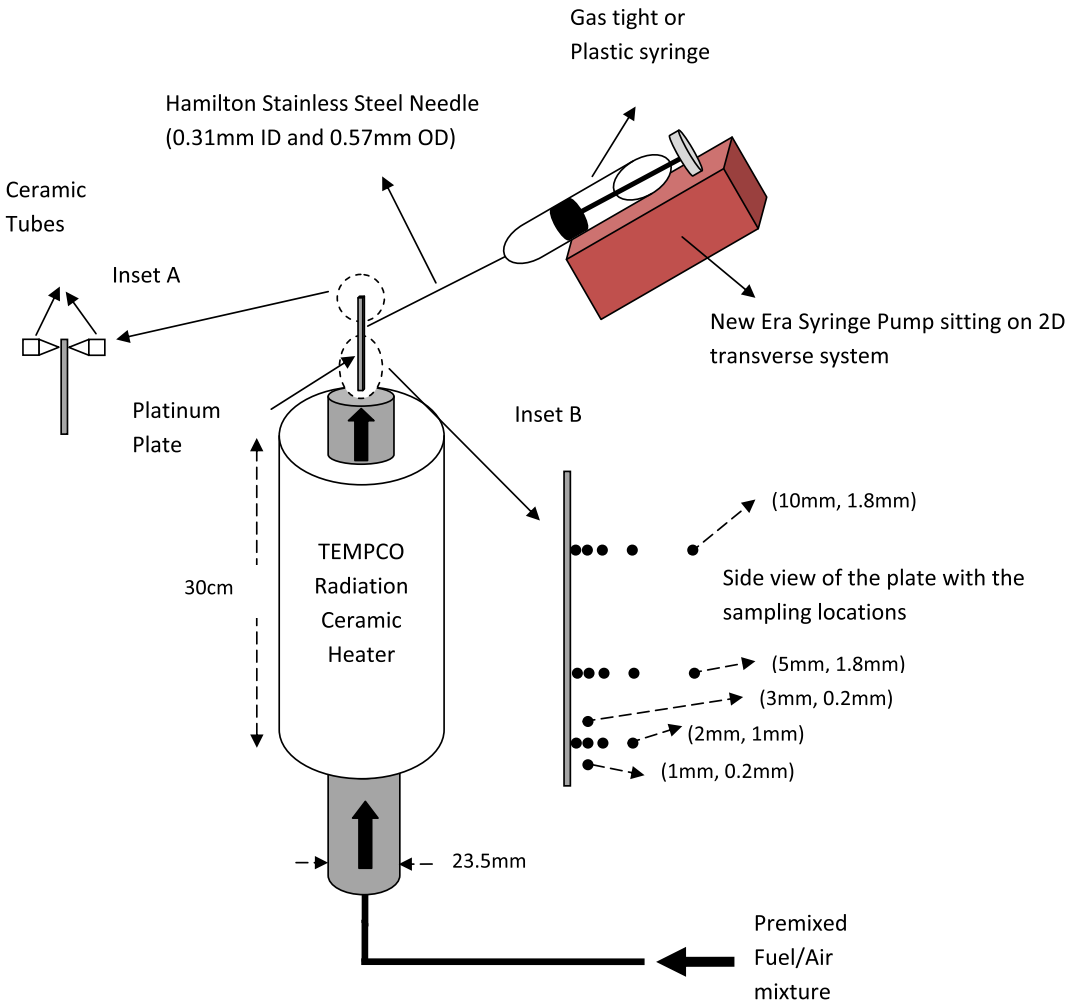

Fig. 1. Gas sampling experimental set up showing the contact mechanism between the platinum plate and the ceramic holders as well as the sampling experimental locations.

Table 1
The streamwise and transverse coordinates of the 16 locations selected for gas analysis.

Transverse location (mm)	Streamwise locations (mm)				
	1	2	3	5	10
0		Location # 2		Location # 7	Location # 12
0.2	Location # 1	Location # 3	Location # 6	Location # 8	Location # 13
0.5		Location # 4		Location # 9	Location # 14
1		Location # 5		Location # 10	Location # 15
1.8				Location # 11	Location # 16

rate of 4 ml/min, a sample of 40 ml is withdrawn. It should be noted here that the suction rate of 4 ml/min was selected from a range of tested rates to minimize disturbance of the boundary layer. The gas samples are now ready for analysis which occurs within a maximum of 2 h from sample collection. The leakage rates from the syringes during this storage time were found to negligible.

Before entering the GC, the gas samples must pass through a Perma Pure Dryer to remove all liquid water and water vapor. The gas sample exiting the Perma Pure Dryer is then delivered to a micro Gas Chromatogram (GC) (Varian CP-4900) where the concentrations of CH_4, C_2H_2, C_2H_6, C_2H_6O, C_3H_6, C_3H_8, C_4H_{10}, O_2, CO_2, CO, H_2, and He will be determined. The micro GC is equipped with two independent analysis modules. Each module extracts a small amount of the sample flow using separate internal sample pumps. CH_4, C_2H_2, C_2H_6, C_2H_6O, C_3H_6, C_3H_8, C_4H_{10}, and CO_2 can be analyzed directly on an 8 m PoraPlot Q (PPQ) column. Some species, such as C_4H_{10} and C_2H_6O, require a specific set of conditions for the PPQ column for them to be detectable. These conditions are referred to as PPQ (high temperature). The separation of O_2, CH_4, CO, H_2, and He are achieved on a 10 μm Molecular Sieve 5A (MS-5A) column.

The GC is calibrated by using special gas calibration cylinders with known concentrations of the gases. The mixture is fed to the GC and the signal is recorded. Then the mixture is diluted with nitrogen, fed to the GC again, and the signal is recorded. This is done for each species of interest. Three or four calibration points are completed for each species and joined by a linear fit that passes through the origin. Based on the average absolute discrepancy obtained in the calibration, as well as the uncertainty of the gas cylinder (2%), mass flow controllers (2%), and micro GC (2%), a relative error <6% is estimated for the measurements of CH_4, C_2H_2, C_2H_6, C_3H_6, C_3H_8, C_2H_6O (DME), C_4H_{10}, O_2, CO_2, CO, H_2, and He.

The procedure to correct for water removal from the sample and recovering the wet-based mole fractions requires the presence of an inert tracer in the sample. In addition to nitrogen, a second

inert tracer was introduced by adding approximately 5% by volume of helium to the premixed fuel/air mixture. The following procedure is then followed in the analysis:

- Three conversion factors, F_i were generated using nitrogen, helium or carbon, respectively as conserved scalars. These are obtained from the ratio of the number of moles in the products, $n_{i,P}$ and reactants, $n_{i,R}$ as follows: for helium ($F_{He} = n_{He,P}/n_{He,R}$), nitrogen ($F_{N2} = n_{N2,P}/n_{N2,R}$) and carbon ($F_C = \Sigma n_{C,P}/\Sigma n_{C,R}$).
- The measured number of moles for all species was corrected by one of these factors and the number of moles of water is then deduced by performing an atomic balance for hydrogen (H). New wet-based mole fractions, based on total number of moles are then obtained.

Several tests were performed using the three different conversion factors, and it was found that F_{N2} based on nitrogen is the most reliable. Significant thermal diffusion of helium was introducing bias in F_{He} and potential carbon loss due to soot precursors may be affecting F_C particularly for rich samples.

Therefore all measurements reported in this paper use the conversion factor obtained from nitrogen as the inert tracer (F_{N2}). The maximum experimental uncertainty in the reported number of moles of oxygen, carbon, and hydrogen to carbon (H/C) ratio is of the order of 15%.

3. Numerical set up

The numerical domain is modeled in a 2D geometry that is shown in Fig. 2. It extends for 20 mm in the x direction and 6 mm in the y direction and is meshed using 10,500 quadratic grid cells. A symmetry boundary condition is applied along the center of the plate which is therefore represented as having a half-thickness of 0.125 mm in order to reproduce the dimensions of the experiment. The inlet boundary condition is taken as a flat velocity profile to match the experimental conditions. The leading edge of the plate is located 1 mm above the jet exit plane. The boundary condition at the trailing edge of the plate (downstream) is modeled as a pressure outlet. This is justified for such configurations where flow reversal may occur within the first few time steps. The boundary opposite the plate surface was set to symmetry since it is far away from the reaction zone. The overall extent of the numerical domain (6 mm × 20 mm) is suitable and further extensions were found to yield no changes in the computed flame structure.

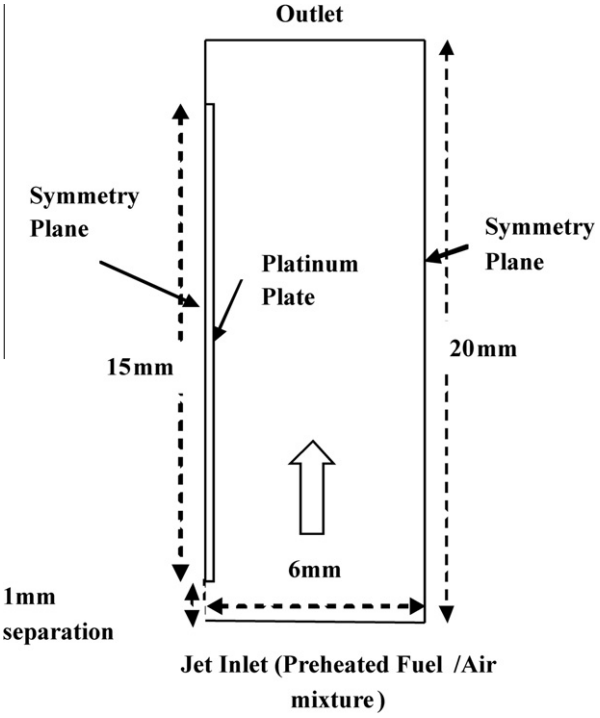

Fig. 2. 2D numerical modeled domain with dimensions and boundary conditions.

The commercial package FLUENT-13 [29] is used in all calculations shown here. A comparison of three different meshes (not shown here) has confirmed that 10,500 quadratic grid cells are sufficient to yield a grid independent solution and hence used in all runs reported here. Gas phase reactions are not used because no propylene/air gaseous chemistry that can be accommodated within the code could be found. The CFD code has a limitation of 50 species for the mechanism to be implemented. Surface chemistry for propylene over platinum is represented by Deutschmann's [3] mechanism which include the following species: Pt(S), O(S), C_3H_6(S), H(S), H_2O(S), CO_2(S), CO(S), NO(S), N(S), C_3H_5(S), C_2H_3(S), CH_2(S), CH_3(S), OH(S), CH(S), C(S), C_3H_5(S2), C_3H_4(S2), C_3H_3(S2), C_2H_2(S2), CH(S2), CHO(S), and C_2H_3O(S). This surface chemistry was developed for three way catalytic convertor (TWC). The GRI2.11 transport database is used along with a comprehensive thermodynamic database accounting for the relevant gaseous and surface species. Unless otherwise stated, all calculations presented here use full thermal and multi-component diffusion. Radiation heat losses at the platinum plate are computed using the Discrete Ordinates (DO) radiation model. It is known that the emissivity of platinum (ε) varies with surface temperature and increases from $\varepsilon = 0.1$ at a temperature of 550 °C to $\varepsilon = 0.19$ at 1500 °C [30]. A fixed value for the emissivity, $\varepsilon = 0.15$ which corresponds to a temperature of 1200 °C is adopted here for convenience. This is considered to be adequate since 1200 °C is close to the average temperature experienced by the platinum during the experiments reported here. It should be noted that, as the emissivity increases, the computed peak temperature decreases but the overall shape of the computed profiles remains unchanged .The calculations for radiation are performed at every flow iteration. Note that the energy equation is solved within the solid plate so that heat conduction can be modeled in both x and y directions (2D). The platinum plate has thermal conductivity of 71.6 W/m K. To identify the impact of gravity on the results presented here, separate calculations accounting for buoyancy revealed negligible effects hence justifying its neglect is subsequent calculations. More detailed descriptions of the models, solvers, and numerical processes used to perform the calculations may be found in [2].

Deutschmann's [3] propylene surface mechanism forces the propylene adsorbed species (C_3H_6(s)) to occupy two empty sites on the surface. The option of multiple site occupancy is not available in FLUENT 13 [29], so the CHEMKIN-CFD [31] package is employed to solve the chemistry part of the solution. CHEMKIN-CFD is a built-in package within FLUENT and it uses the same methodology as the CHEMKIN software to solve the chemistry. The absolute and relative convergence tolerances used for the surface and gaseous species are set to 10^{-12} and 10^{-6}, respectively. Pseudo-time stepping is set to 10^{-6} s with the maximum and minimum set to 10^{-4} s and 10^{-12} s, respectively.

4. Experimental results

4.1. Platinum plate temperature and reactivity limits

Measured profiles of the peak temperature of the platinum surface reacting with propylene/air mixtures, $T_{P,max}$, are presented in

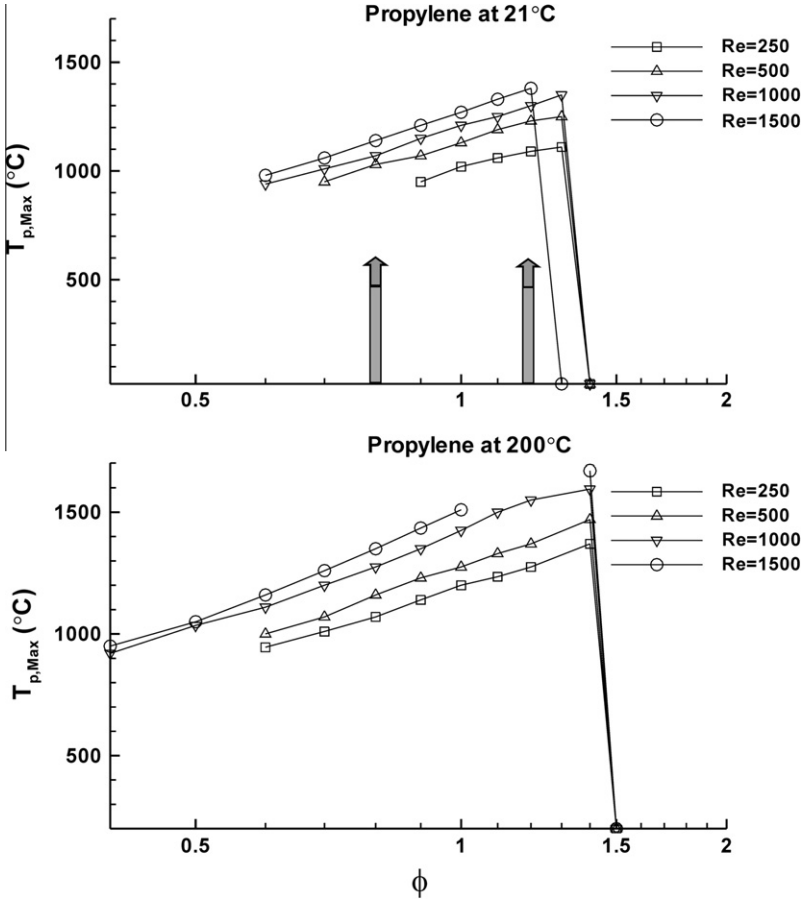

Fig. 3. Maximum measured surface temperature vs. equivalence ratio Φ (on a logarithmic scale) for propylene at different values of T_{jet} and Re. Vertical bars and arrows point to the equivalence ratios for species analysis.

Fig. 3 vs. equivalence ratio (note the logarithmic scale). Results are shown for Reynolds numbers ranging from 250 up to 1500 and for initial approach temperatures of 21 °C, and 200 °C. This was a limiting case since temperatures higher than 200 °C led to auto-ignition within the steel pipe. The following observations are made:

- Regardless of the temperature of the incoming propylene/air mixture (T_{jet}), the maximum peak plate temperature for flameless combustion occurs at moderately rich mixtures of $\Phi = 1.3$ at $T_{jet} = 21$ °C and of $\Phi = 1.4$ at $T_{jet} = 200$ °C. Also, for the flameless combustion mode, the peak plate temperature increases with increasing Reynolds numbers and T_{jet}. For example, using propylene/air at $T_{jet} = 21$ °C, the peak platinum temperature at $\Phi = 1.3$ increases from 1110 °C at Re = 250–1380 °C at Re = 1500. It should be noted that this behavior is consistent with that reported earlier for other fuels [2].
- The discontinuity in the peak plate temperature profile for propylene/air mixture at $T_{jet} = 200$ °C and Re = 1500 in Fig. 3, refers to the situation where a gaseous flame engulfs the platinum (flaming combustion). Under these conditions, the flame is blown off straight away so it does not cause damage to the platinum plate.
- Rich propylene/air mixtures (Fig. 3) undergo a very sharp transition to extinction regardless of the Reynolds number and this occurs at $\Phi = 1.4$ for $T_{jet} = 21$ °C and at $\Phi = 1.5$ for $T_{jet} = 200$ °C. This transition from a highly reacting plate to extinction is mostly independent of the Reynolds number and may be due to the formation of soot precursors which may contaminate the platinum by occupying the active sites and hence causing extinction. While this only a speculation, it is well known that propylene is one of the sootiest fuels amongst the alkenes and is definitely sootier than the alkanes [32].

The reactive limits for propylene are presented in Fig. 4 as plots of equivalence ratio vs. the Reynolds number for various fuel mix-

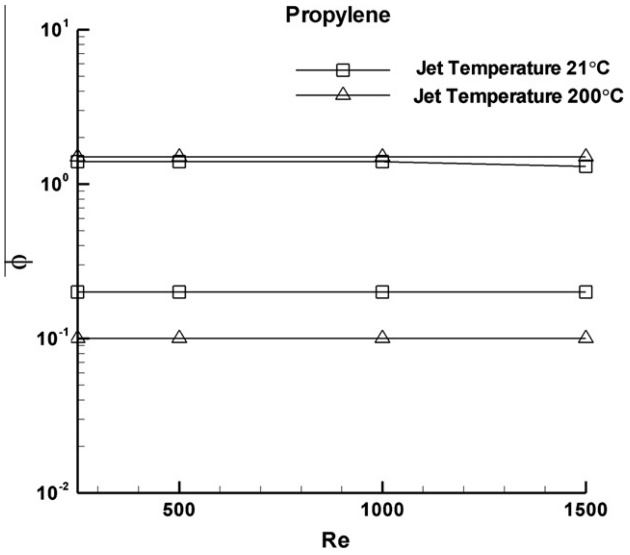

Fig. 4. Plots of Φ vs. Re on a log–log scale showing the experimental lean and rich reactive limits of propylene/air mixtures over platinum and for different values of T_{jet}.

Table 2
Conditions of the propylene/air cases selected for gas analysis.

Case #	T_{jet} (°C)	Re	Velocity (m/s)	Φ	He (%) in reactants
1	21	500	0.32	0.8	4.08
2	21	500	0.31	1.21	4.06
3	21	1000	0.63	1.17	4.36
4	200	500	0.77	1.26	4.33

ture temperatures (T_{jet}). Note that the Φ axis shows a logarithmic scale. Lean and rich reactive limits (Φ_L, Φ_R) are presented for each value of T_{jet}. It should be noted that these limits were determined from temperature measurements obtained using either a pyrometer (for temperatures 700–2000 °C) or a thermocouple placed on top of the platinum plate. The reactive limits are defined as the condition when the temperature rise decreases to nearly zero, i.e. when the temperature of the platinum (or the gas downstream of it, if measured by the thermocouple) drops to that of the incoming fuel mixture stream. A comparison between the reactivity limits from this study and the gaseous flammability limits is also made. The gaseous flammability limits are either found in literature or calculated using the correlation developed by Zabetakis [33]. The following observations are noted:

- The lean reactive limits, Φ_L, are generally independent of the Reynolds number and decrease with the increasing temperature of the mixture. This statement is true also for gas phase mixtures but the lean reactive limit in the presence of platinum is

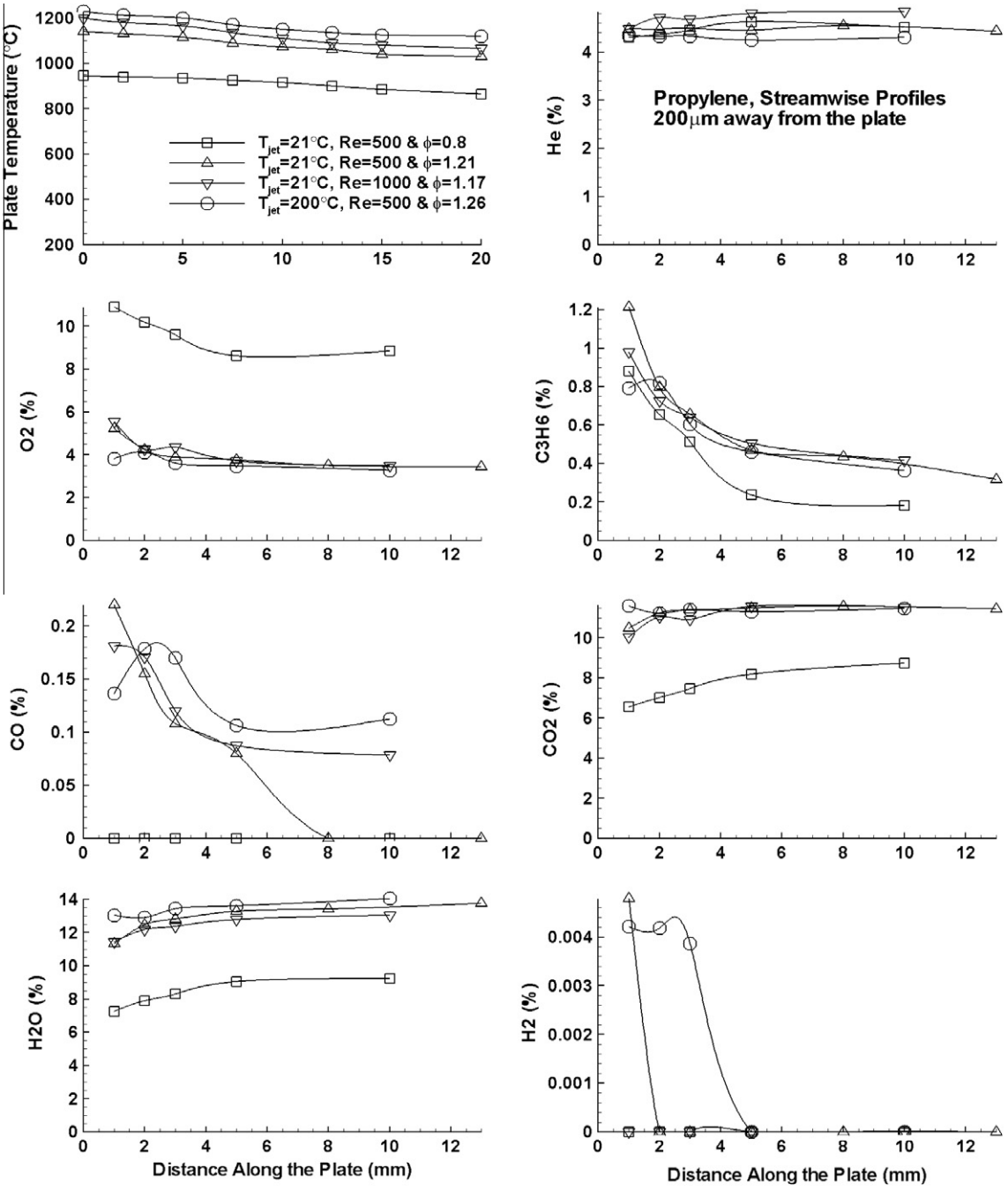

Fig. 5. Streamwise profiles of the temperature and He, O_2, C_3H_6, CO, CO_2, H_2O, and H_2 wet-based mole fractions 200 μm away from the plate for Cases 1, 2, 3, and 4 using propylene/air mixtures.

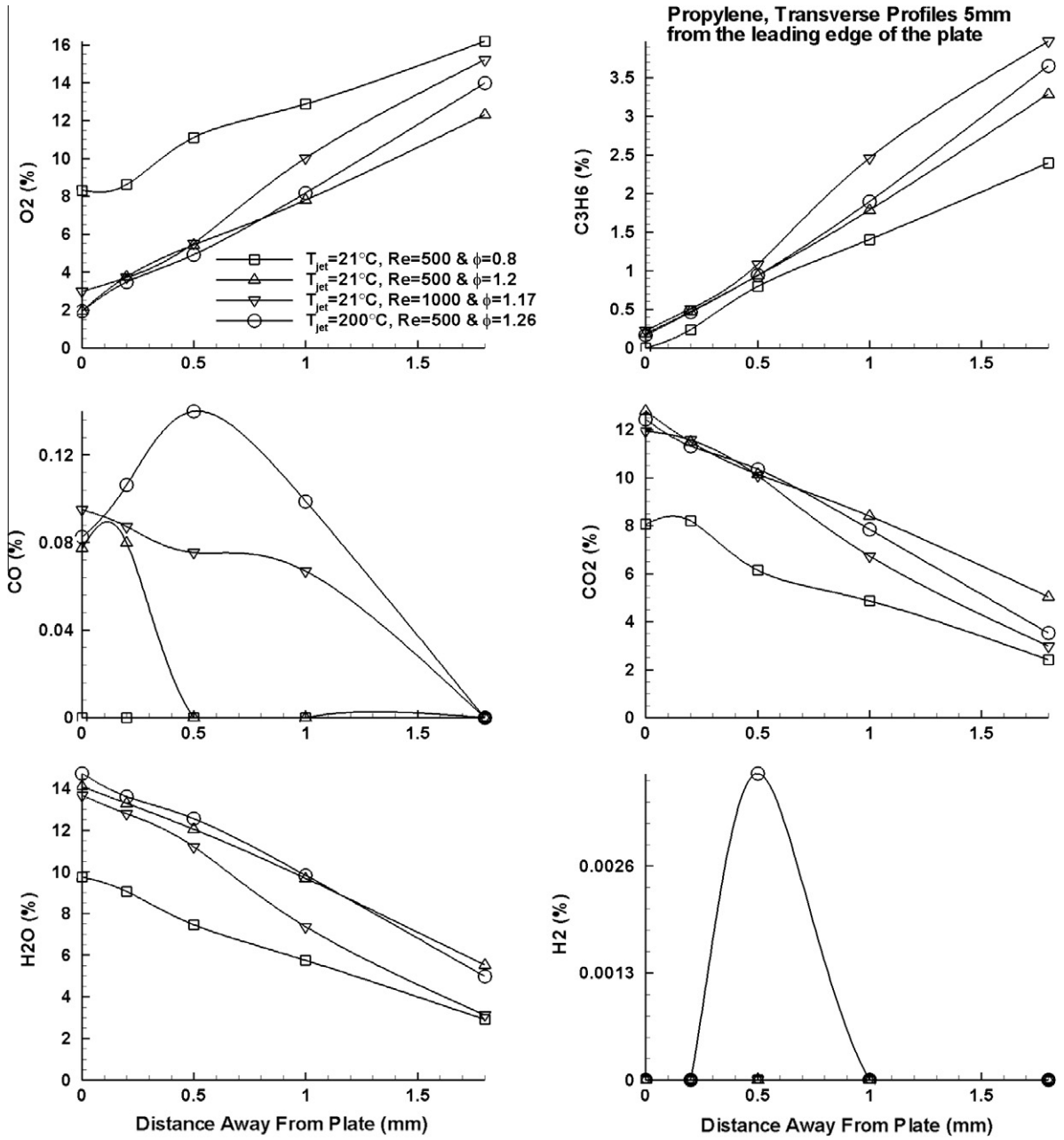

Fig. 6. Transverse profiles of O_2, C_3H_6, CO, CO_2, H_2O, and H_2 wet-based mole fractions 5 mm downstream of the leading edge of the plate for Cases 1, 2, 3, and 4 using propylene/air mixtures.

always lower than the corresponding gaseous limit ($\Phi_{L,\ gas\ phase}$). For example, the lean limits for a propylene/air mixture at T_{jet} = 21 °C and Re = 250 are 0.2 and 0.44 with and without the presence of a platinum plate, respectively. It should be noted that the degree of broadening in the reactive limits of propylene on platinum will vary with system parameters such as heat losses by radiation.

- The rich reactive limits, Φ_R, shown in Fig. 4 are almost uniform with Reynolds number and these, in turn, are lower than the rich limits of gaseous mixtures of the same fuel at the same temperature. A propylene air mixture at T_{jet} = 21 °C and Re = 250 experiences extinction at Φ_R = 1.5 when platinum is present and at $\Phi_{R,\ gas\ phase}$ = 2.64 when burning propylene/air homogeneously. This observation points to potential poisoning of the surface by soot precursors such as polycyclic aromatic hydrocarbons.
- The trend observed is that Φ_R increases at higher T_{jet} values regardless of the Reynolds number. However, the dependence on T_{jet} is minimal since the rich reactive limit for the propylene/air mixture increases from 1.4 at T_{jet} = 21 °C to 1.5 at T_{jet} = 200 °C.

4.2. Product species analysis

Propylene/air mixtures selected for product species analysis are described in detail in Table 2. The selected cases cover a range of Φ, Re, and T_{jet} and their location in equivalence ratio space is marked by the vertical bars shown in Fig. 3. The reference Reynolds number is taken as 500 and the reference inlet temperature is taken as 21 °C. The approach velocities at the exit plane of the burner, near the leading edge of the plate are also tabulated. Two different equivalence ratios (Cases 1, and 2) are tested at the reference Re and T_{jet}. Case 3 is at the reference temperature (21 °C) but with a

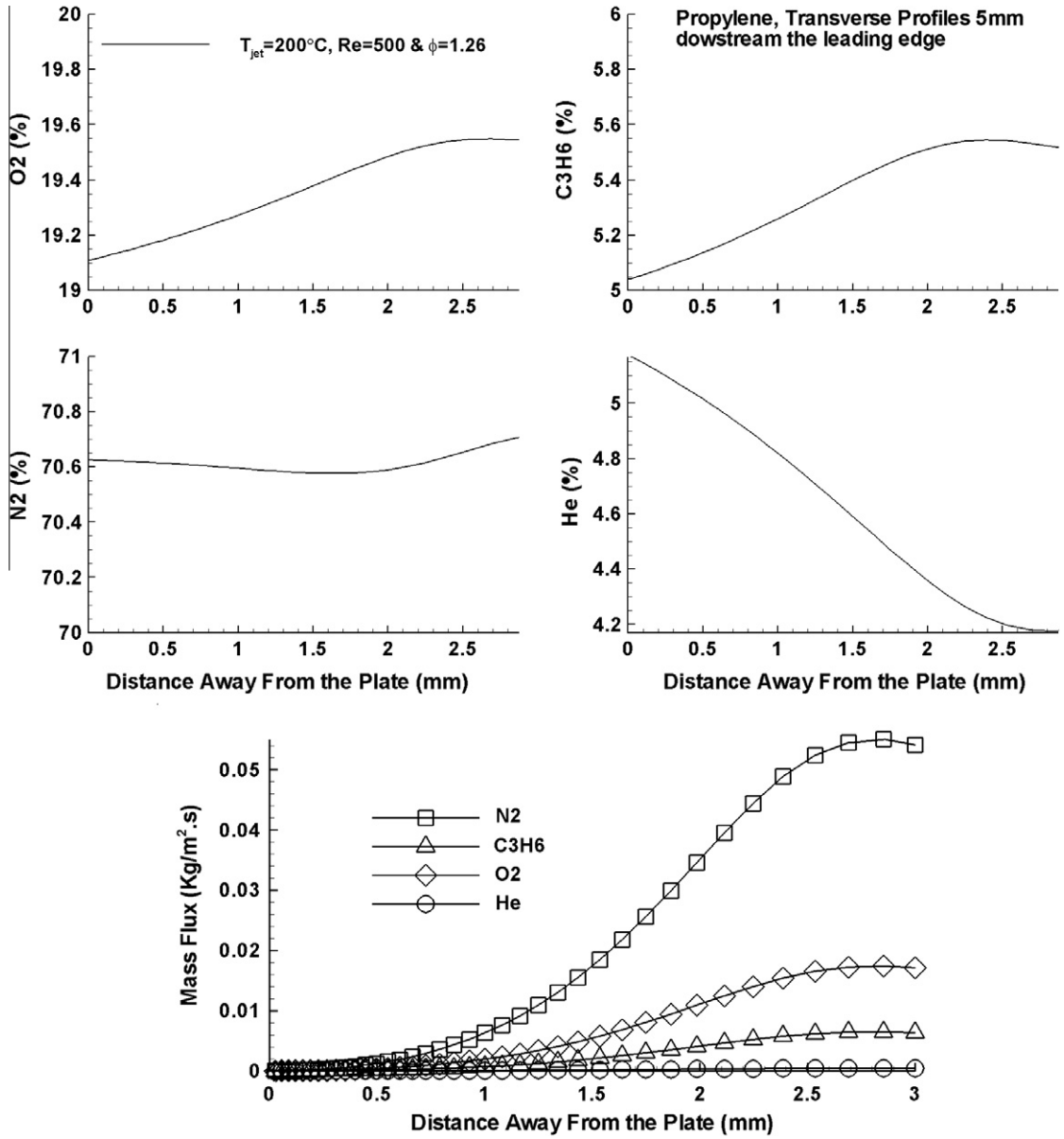

Fig. 7. Numerical transverse profiles of O_2, C_3H_6, N_2, and He mole fractions calculated 5 mm downstream the leading edge of a heated, non-reacting plate. Also shown in the lower plot are the transverse mass fluxes of these species computed at 5 mm from the leading edge.

higher Re, while Case 4 studies the effect of T_{jet} by having Re at the reference value (500). An equivalence ratio higher than 1.2 could not be tested because extinction occurs in this vicinity.

For comparison purposes, the streamwise (200 μm away from the plate) and transverse profiles of the species are measured and plotted for different cases. Figure 5 shows streamwise profiles measured at 200 μm away from the platinum plate for temperature and the wet-based mole fractions of He, O_2, C_3H_6, CO, CO_2, H_2O, and H_2. Results are presented for Cases 1–4 on each plot and several observations can be drawn:

- The temperature decreases only slightly along the length of the plate and the decay between the leading and trailing edges is around 100–150 °C for all cases shown here. This trend is similar to the findings noted earlier for other fuels [33] but is inconsistent with the results of Smyth et al. [20,21] which showed a much more significant decay in temperature possibly due to higher heat losses to the plate holders.
- The main combustion products are CO_2 and H_2O. Carbon monoxide and hydrogen exist in very small amounts mostly in the leading edge region and decay further away from of the plate as do O_2 and C_3H_6. The structure of the boundary layer along the plate is consistent with that noted earlier [20,21] and consists of two nominal zones defined as: (i) the leading edge zone (0 mm to about 5 mm from the leading edge of the plate) where gradients of species are observed and (ii) the trailing edge region (5–10 mm from the leading edge) where the streamwise profiles of species are somewhat flat and more uniform.
- Oxygen decreases significantly as the equivalence ratio increases, but the remaining species increase with the equivalence ratio at different rates. Oxygen is nearly halved when Φ rises from 0.8 to 1.21. Carbon monoxide and hydrogen do not appear in the products for the lean case (Case 1 in Table 2), but they are present in low quantities for the slightly rich case (Case 2 in Table 2) at the leading edge of the plate. Note that CO is detected 5 mm

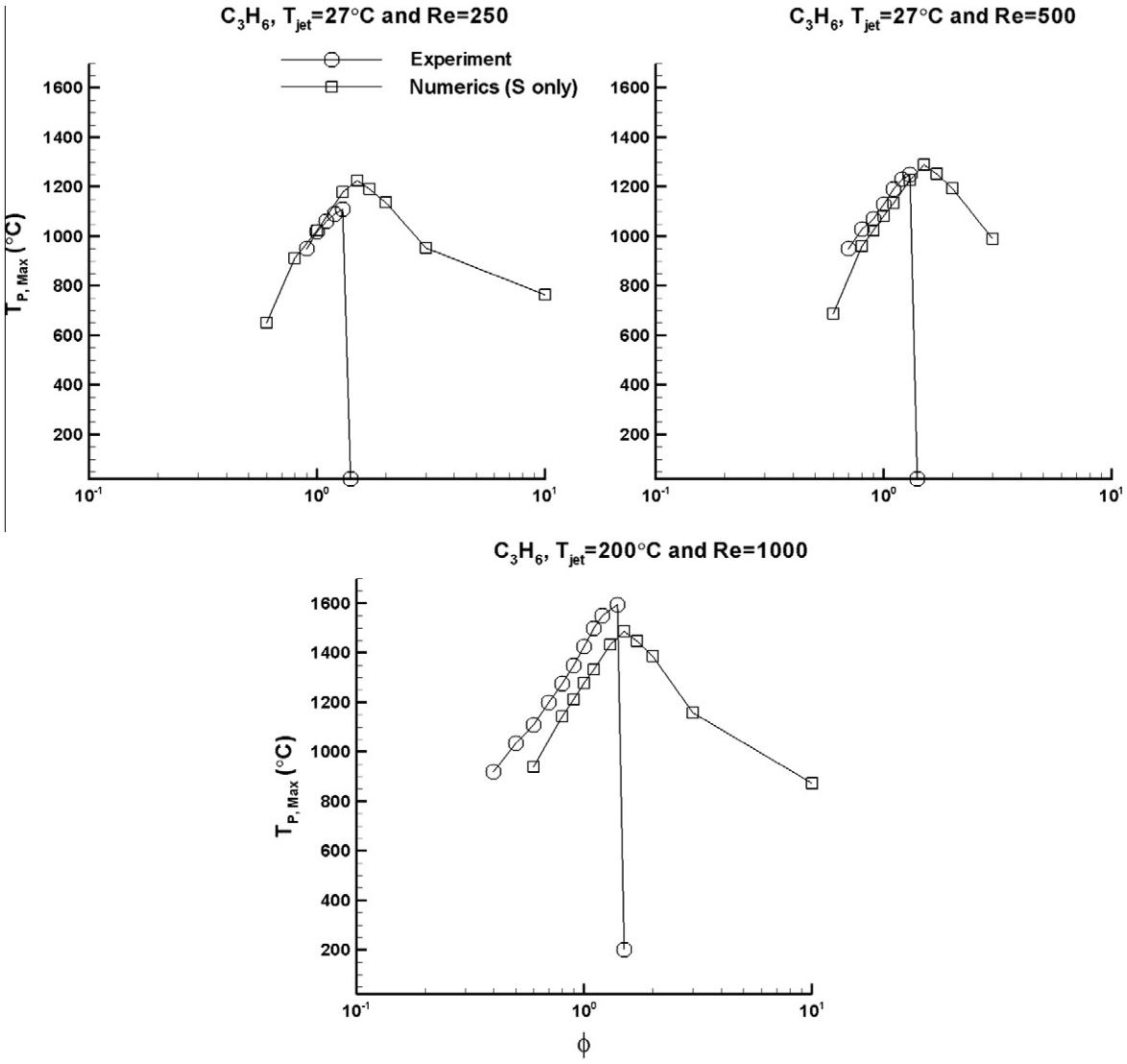

Fig. 8. Maximum measured surface temperature plotted vs. equivalence ratio Φ (on a logarithmic scale) for propylene/air mixtures over platinum: Numerical predictions (surface chemistry only) compared with experimental data for various flow conditions.

from the leading edge. Hydrogen extends further downstream (3 mm from the leading edge) for higher T_{jet} (Case 4 compared to Case 2) and disappears completely when Re increases from 500 to 1000 (Case 3 compared to Case 2).

- Carbon dioxide and water increase significantly as Φ increases from 0.8 to 1.21. Almost a 50% increase is observed for CO_2 and H_2O along the length of the plate, with the mole fractions of the products in the rich case consisting of about 12% H_2O and 11% CO_2.

The transverse profiles of the temperature of the species wet-based mole fractions for all cases shown in Table 2 are presented in Fig. 6 at 5 mm downstream the leading edge of the plate. Transverse profiles of the species at 2 mm, and 10 mm from the leading edge are also available but not shown here. The same conclusions from the previous discussion apply, but the transverse profiles highlight the following additional points:

- As expected, oxygen and fuel increase away from the plate and the product mole fractions decrease as the desorbed species are gradually mixed with the surrounding gases in the boundary layer.
- The fuel is almost fully consumed on the surface even for the rich case with $\Phi = 1.21$ while O_2 mole fractions remain relatively high. This is partly due to preferential differential and thermal diffusions which result in mixtures closer to the plate leaner than those in the free-stream (this issue is further discussed later in the paper). A corollary of this effects is the low selectivity to CO and H_2 even for these rich mixtures ($\Phi = 1.21$) and fuel conversion to CO_2 and H_2O is almost complete with negligible amounts CO and H_2 present.
- Peaks in CO and H_2 profiles may develop away from the plate at different transverse locations, especially when $T_{jet} = 200$ °C. Hydrogen peaks at the plate surface at 2 mm from the leading edge (not shown here) and then further downstream, at 5 mm, the peak shits to 0.5 mm away from the plate marking a potential contribution from the gas-phase chemistry. It is also worth noting that hydrogen appears to be fully consumed at 10 mm downstream of the leading edge while CO (not shown) remains albeit in lower volume fractions.

5. Numerical results

The higher helium and oxygen mole fractions measured near the plate, as well as the difference in the water deduced from

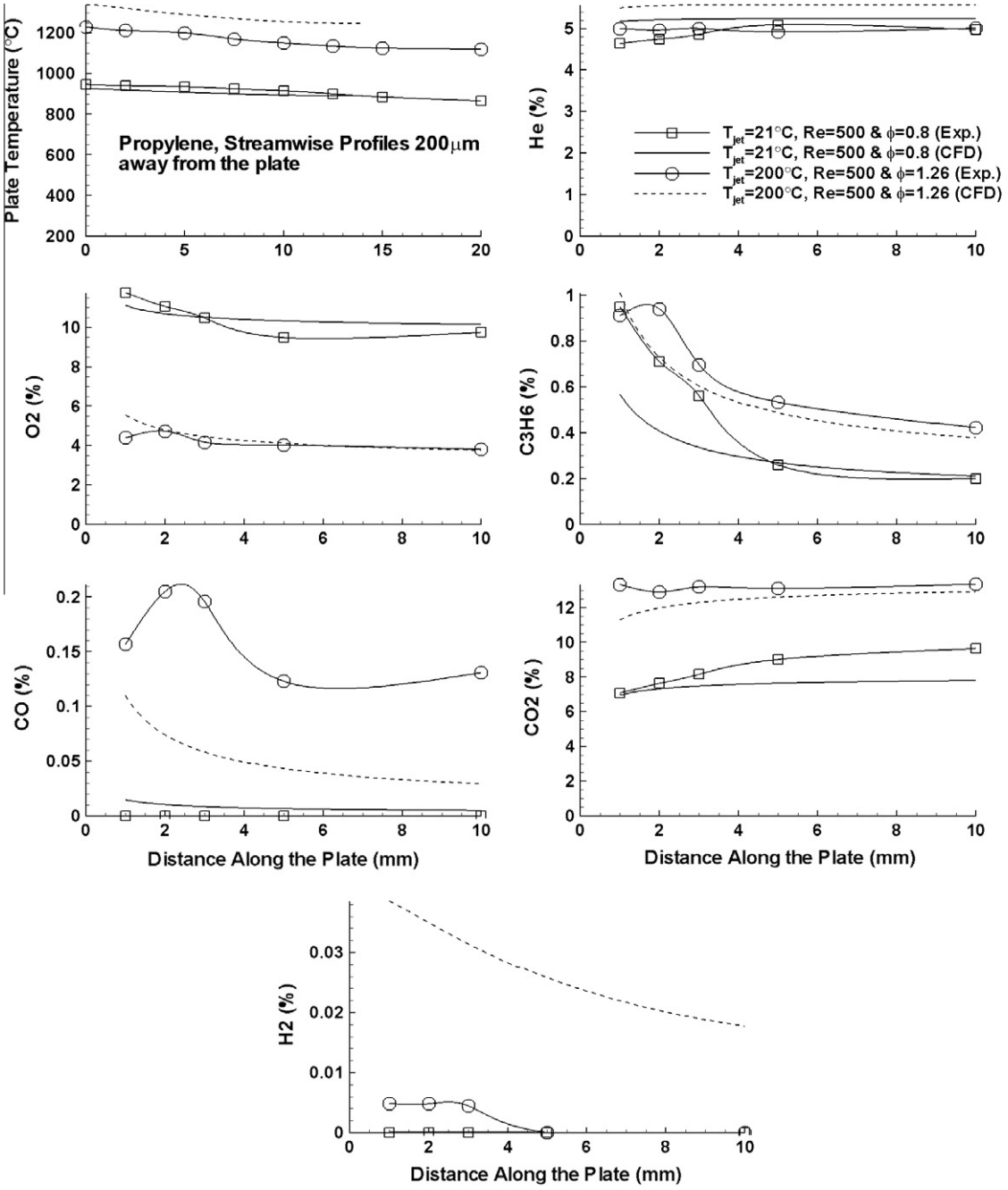

Fig. 9. Experimental vs. CFD streamwise profiles of the temperature and He, O_2, C_3H_6, CO, CO_2, and H_2 dry-based mole fractions 200 μm away from the plate for Cases 1, and 4 using propylene/air mixtures.

the balance of hydrogen and oxygen atoms fraction point to the significant role of differential molecular diffusion and, potentially, thermal diffusion. The contribution of thermal diffusion is examined numerically for a non-reacting case of fuel–air–helium mixture ($\Phi = 1.26$) at 200 °C inlet temperature (T_{jet}) flowing near a heated plate. The temperature of the plate is maintained at 1600 K which is similar to the temperature measured in the cases presented here. Figure 7 shows transverse profiles of the computed mole fractions of the various species at 5 mm from the leading edge. The effects of thermal diffusion are evident with helium mole fraction near the plate increasing by more than 20% and the mole fractions of fuel and oxygen decreasing by about 10% and 2% respectively. This thermal diffusion clearly results in leaner mixtures near the plate and renders the hydrogen and carbon balance invalid. This explains some of the inadequacies noted earlier with the water mole fractions deduced from the measurement so to circumvent this problem, further comparisons between measurements and calculations are performed on a dry-basis only.

The mass fluxes of few species are plotted in Fig. 7 to confirm that the mass fluxes of all species in the non-reacting case are approaching zeros at the wall of the plate. This is clearly seen from the transverse profiles of the mass fluxes presented in Fig. 7. The mass flux of species i is calculated using the expression $\dot{m}_i' = \rho Y_i V_n$, where ρ is the density, Y_i is the mass fraction of species i and V_n is the velocity component that is normal to the plate. While the effect of differential molecular diffusion could not be isolated numerically because of the limitation of the software, it

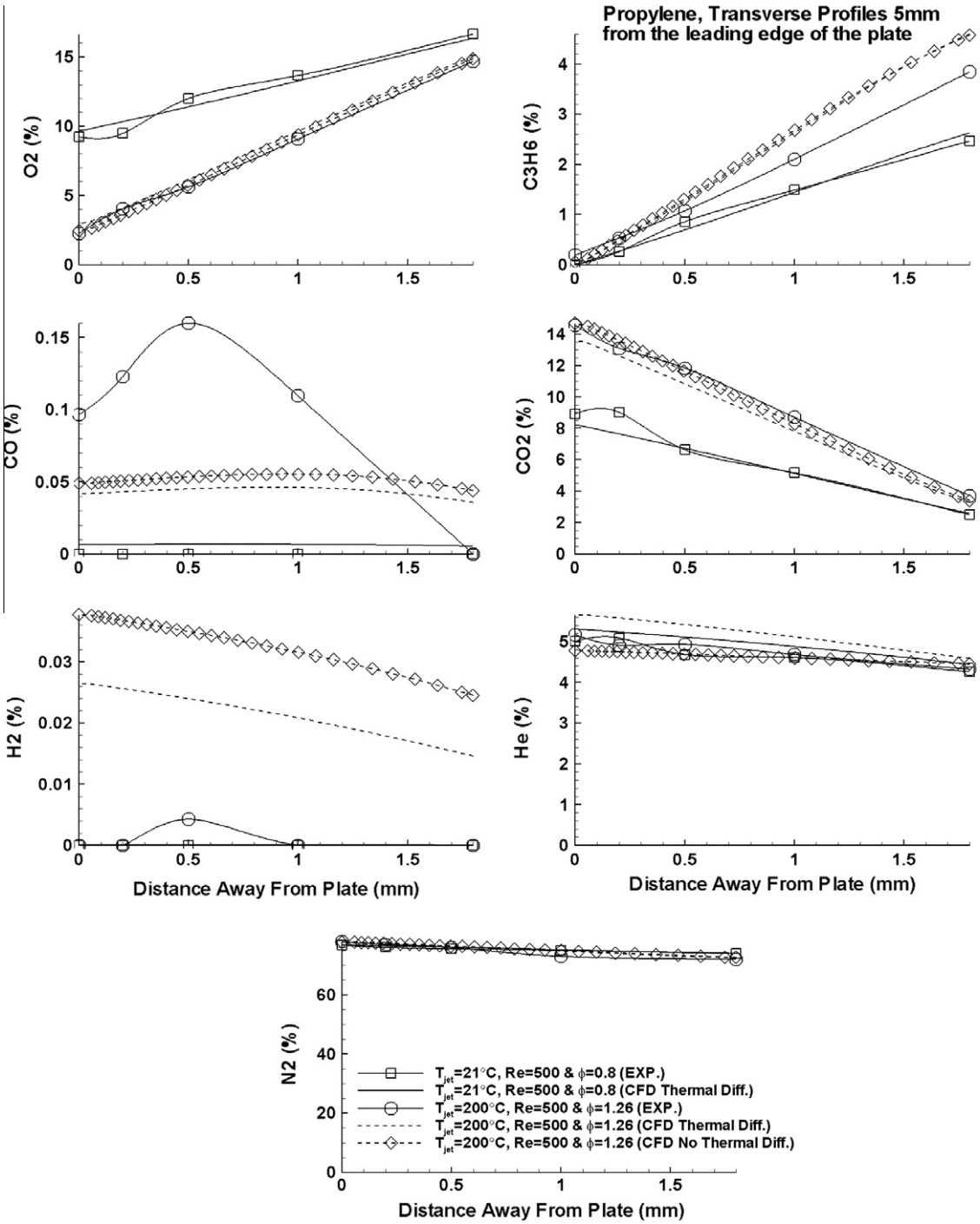

Fig. 10. Experimental vs. CFD transverse profiles of O_2, C_3H_6, CO, CO_2, H_2, He, and N_2 dry-based mole fractions 5 mm from the leading edge of the plate for Cases 1, and 4 using propylene/air mixtures.

is believed that this effect is significant and outweighs thermal diffusion. This has been confirmed by Appel et al. [7] who performed a study on the homogeneous ignition of hydrogen on platinum and isolated the effects of Fickian and thermal diffusion. They reported that Fickian diffusion is dominant and thermal diffusion has a minor impact on the imbalance of hydrogen near the plate. A similar conclusion is expected to apply here.

A comparison is first made between the measured and computed maximum plate temperature, $T_{p,max}$, as shown in Fig. 8 for three propylene/air cases, namely $T_{jet} = 27\ ^\circ C$ for Re = 500 and 1000 and $T_{jet} = 200\ ^\circ C$ and 1000. The results are plotted vs. the equivalence ratio Φ using a logarithmic scale. The emissivity of platinum used in the calculations is 0.15 and this is consistent with what has been used earlier [2] where it has also been established that there is insignificant difference between 2D and 3D calculations. Good agreement is noted for equivalence ratios less than $\Phi \sim 1.4$. The lean reactive limits, which are lower than the limits for gaseous propylene/air mixtures, are also adequately reproduced. At equivalence ratios larger than $\Phi \sim 1.4$, the calculations show a continuous decrease in $T_{p,max}$ and fail to compute the sudden extinction limit that has been observed experimentally. This is consistent with the hypothesis that the soot is causing the

extinction of reactions on the platinum plate because the numerical surface chemistry used here does not account for soot formation and hence will not compute this extinction. The increase of $T_{p,max}$ with increasing Reynolds number is reproduced numerically as shown from the top two plots in Fig. 8. However, the discrepancy between the measured and computed $T_{p,max}$ increases at higher T_{jet} values and this may be due to potential contributions from gas-phase chemistry which is missing from the calculations. This is consistent since the measured $T_{p,max}$ is higher than the calculations for the case with T_{jet} = 200 °C.

For a more detailed comparison with the experimental data, the temperature on the plate surface and the dry-based species concentrations are shown for both measurements and calculations in Fig. 9 for the streamwise profiles and Fig. 10 for the transverse profiles at 5 mm from the leading edge of the plate. Two cases, namely Cases 1 and 4 (see Table 2) are selected here to highlight the adequacy of the results for lean as well as rich propylene/air mixtures. Figure 10 shows additional calculations for the rich case of Φ = 1.23 but without accounting for thermal diffusion. A few observations can be made:

- Consistent with the peak temperatures shown earlier, the computed surface temperature along the streamwise temperature is in good agreement with measured temperature along the entire length of the platinum plate.
- Both streamwise and transverse profiles show adequate agreement for fuel and oxygen as well as the mole fraction CO_2. These consistent trends confirm the presence of two nominal zones along the plate, namely a leading zone extending for about 5 mm from the leading edge followed by a trailing zone.
- Significant disagreement is noted between the measured and calculated mole fractions of carbon monoxide and hydrogen albeit these species are present in low quantities such as 0.015% for CO and 4.5×10^{-5}% for H_2.
- The computed transverse profiles shown in Fig. 10 for 5 mm from the leading edge (as well as others at 2 mm and 10 mm, not shown here) show that despite significant discrepancies with experiments, particularly for CO and H_2, the overall structure of the inner layer close to the platinum surface is adequately reproduced. Note that discrepancies in the outer layer may be largely due to influence of gas chemistry which is not accounted for in the calculations.
- Molecular as well as thermal diffusions are clearly changing the species balance on the plate with helium being higher than in the free stream while CO_2 and H_2 are lower than the case where thermal diffusion is disabled. Nitrogen is not affected and this confirms its selection (instead of helium) as a conserved scalar in data processing. This is consistent with the results shown earlier for the case of a heated plate and confirms that thermal diffusion is significant and leads to lower equivalence ratios near the plate than those injected in the free stream.

6. Discussion

While the interactions of propylene with platinum possess qualitatively similar features to those reported earlier for other hydrocarbon fuels [1,2], subtle differences exist as reported in this paper and noted here. The levels of CO formed in the boundary layer are generally lower than those reported for ethane and much lower than the CO levels formed with platinum-methane interactions. The most distinct feature, however, is the narrow rich reactive limits obtained over all Reynolds numbers and in-flow temperatures. The hypothesis that this is caused by soot precursors contaminating the platinum surface and "switching off" reaction is supported by the very narrow range of equivalence ratio over which this extinction occurs. This is very consistent with the reported equivalence ratios where soot nano-particles start to form in abundant concentrations [34]. Future work should further explore the correlation between this rich extinction limit and soot formation.

Calculations of the structure of the boundary layer, while adequate for the cases shown here, highlight the need for further developments in the surface chemistry of propylene on platinum. A sensitivity analysis, particularly for species such as CO and H_2 which show significant deviations from experiments would be useful to identify key reactions that should be targeted for further studies. In fact, this need for improvement is true for surface chemistry in general starting with the generation of reliable thermodynamics bases for surface-active species similar to those generated for gaseous species. The use of combined gaseous and surface chemistries would be relevant to reproduce some of the hetero-homogeneous interactions that were highlighted in the measurements. However, the prediction of the rich reactive limits may prove to be difficult as this is likely to require the inclusion of complex kinetics that accounts for the formation of soot precursors.

7. Conclusions

Measurements and calculations of surface temperature and species mole fractions are performed for premixed propylene/air mixtures reacting over platinum. The effects of the jet temperature (T_{jet}), equivalence ratio (Φ), and the Reynolds number of the issuing gas (Re) on the reactivity are investigated. The following conclusions are drawn:

- The temperature of the platinum increases with increasing Re and T_{jet} and peaks at moderately rich propylene/air mixtures (Φ = 1.3) before transitioning sharply to extinction at slightly richer mixtures of Φ = 1.5. This is lower than the corresponding rich limit for gaseous propylene-air and the reduction may be due to the contamination of platinum by soot precursors.
- The main products of burning propylene/air mixtures over platinum are CO_2, and H_2O. Carbon monoxide and H_2 appear in low quantities in the products and for certain flow conditions.
- Two reactive zones along the plate are observed: a leading edge zone stretching for about 5 mm from the leading edge and a trailing edge zone covering the rest of plate. Gradients in species mole fractions are detected at the leading edge zone while flat profiles of species are generally noted within the trailing edge regime.
- Good agreement is obtained between the calculated and measured surface temperatures of the plate. Species such as oxygen (O_2), propylene (C_3H_6), and CO_2 are in good agreement with the measured mole fractions while CO and H_2 show some discrepancies.
- Differential molecular as well as thermal diffusions are found to play significant roles in changing the species concentrations leading to mixtures close to the surface of the plate that are leaner than those injected in the free stream.

References

[1] J. Badra, A.R. Masri, C. Zhou, B.S. Haynes, Fuel, http://dx.doi.org/10.1016/j.fuel.2012.08.021.
[2] J.A. Badra, A.R. Masri, Combust. Flame 159 (2) (2012) 817–831.
[3] D. Chatterjee, O. Deutschmann, J. Warnatz, Faraday Discuss. 119 (2002) 371–384.

[4] O. Deutschmann, L.I. Maier, U. Riedel, A.H. Stroemman, R.W. Dibble, Catal. Today 59 (1–2) (2000) 141–150.
[5] O. Deutschmann, R. Schmidt, F. Beherendt, J. Warnatz, Proc. Combust. Inst. 26 (1996) 1747–1754.
[6] D.K. Zerkle, M.D. Allendorf, M. Wolf, O. Deutschmann, J. Catal. 196 (1) (2000) 18–39.
[7] C. Appel, J. Mantzaras, R. Schaeren, R. Bombach, A. Inauen, B. Kaeppeli, B. Hemmerling, A. Stampanoni, Combust. Flame 128 (4) (2002) 340–368.
[8] S. Prakash, N.G. Glumac, N. Shankar, M.A. Shannon, Combust. Sci. Technol. 177 (4) (2005) 793–817.
[9] J. Mantzaras, R. Bombach, R. Schaeren, Proc. Combust. Inst. 32 (2) (2009) 1937–1945.
[10] P.A. Bui, D.G. Vlachos, P.R. Westmoreland, Proc. Combust. Inst. 26 (1996) 1763–1770.
[11] J.C.G. Andrae, P.H. Björnbom, AIChE J. 46 (7) (2000) 1454–1460.
[12] Y. Ghermay, J. Mantzaras, R. Bombach, Proc. Combust. Inst. 33 (2011) 1827–1835.
[13] S. Karagiannidis, J. Mantzaras, K. Boulouchos, Proc. Combust. Inst. 33 (2011) 3241–3249.
[14] S. Karagiannidis, J. Mantzaras, G. Jackson, K. Boulouchos, Proc. Combust. Inst. 31 (2) (2007) 3309–3317.
[15] M. Reinke, J. Mantzaras, R. Bombach, S. Schenker, A. Inauen, Combust. Flame 141 (4) (2005) 448–468.
[16] M. Reinke, J. Mantzaras, R. Schaeren, R. Bombach, A. Inauen, S. Schenker, Combust. Flame 136 (1–2) (2004) 217–240.
[17] M. Reinke, J. Mantzaras, R. Schaeren, R. Bombach, W. Kreutner, A. Inauen, Proc. Combust. Inst. 29 (2002) 1021–1029.
[18] S. Karagiannidis, J. Mantzaras, R. Bombach, S. Schenker, K. Boulouchos, Proc. Combust. Inst. 32 (2009) 1947–1955.
[19] G.D. Stefandis, D.G. Vlachos, Ind. Eng. Chem. Res. 48 (2009) 5962–5968.
[20] S.A. Smyth, K.T. Christensen, D.C. Kyritsis, Proc. Combust. Inst. 32 (2009) 3035–3042.
[21] S.A. Smyth, D.C. Kyritsis, Combust. Flame 159 (2012) 802–816.
[22] P. Markatou, L.D. Pfefferle, M.D. Smooke, Combust. Flame 93 (1993) 185–201.
[23] V. Dupont, S.-H. Zhang, R. Bentley, A. Williams, Fuel 81 (2002) 799–810.
[24] R.E. Hayes, S.T. Kolaczkowski, Introduction to Catalytic Combustion, Gordon and Breach Science Publishers, Amsterdam, 1998.
[25] G.J. Griffin, D.G. Wood, Catal. Today 63 (2) (2000) 387–395.
[26] O. Deutschmann, F. Behrendt, J. Warnatz, Catal. Today 21 (2–3) (1994) 461–470.
[27] N.S. Kaisare, S.R. Deshmukh, D.G. Vlachos, Chem. Eng. Sci. 63 (4) (2008) 1098–1116.
[28] L. Ma, D.L. Trimm, C. Jiang, Appl. Catal. A 138 (2) (1996) 275–283.
[29] Fluent 13. <http://www.ansys.com/Products/Simulation+Technology/Fluid+Dynamics/ANSYS+FLUENT> (20.01.12).
[30] Emissivity of Platinum. <http://www.platinummetalsreview.com/jmpgm/data/displayFunctionalGraph.do;jsessionid=40584A142C4D91784CC7BD150B2DF3A4?record=1219&attribute=154&database=cesdatabase> (11.04.11).
[31] CHEMKIN-CFD. <http://www.reactiondesign.com/products/open/kinetics_module.html> (10.03.12).
[32] A. Gomez, J.J. Berry, A. Roychoudhury, B. Coriton, J. Huth, Proc. Combust. Inst. 31 (2007) 3251–3259.
[33] M. G. Zabetakis, Flammability characteristics of combustible gases and vapors, Bureau of Mines, Alaska, 1665a, pp. 22, 23, 70.
[34] A. Schocker, K. Kohse-Höinghaus, A. Brockhinke, Appl. Opt. 44 (31) (2005) 6660–6672.